Inorganic Chemistry

Article

pubs.acs.org/IC

Noncovalent Interactions between a Trinuclear Monofunctional Platinum Complex and Human Serum Albumin

Yanqing Wang,[†,§] Xiaoyong Wang,*[,‡] Jing Wang,[‡] Yongmei Zhao,[†] Weijiang He,[†] and Zijian Guo*[,†]

[†]State Key Laboratory of Coordination Chemistry, School of Chemistry and Chemical Engineering, Nanjing University, Nanjing 210093, P.R. China

[‡]State Key Laboratory of Pharmaceutical Biotechnology, School of Life Sciences, and State Key Laboratory of Analytical Chemistry for Life Science, Nanjing University, Nanjing 210093, P.R. China

[§]Institute of Applied Chemistry and Environmental Engineering, Yancheng Teachers University, Yancheng, 224002, P.R. China

ABSTRACT: Interactions between platinum complexes and human serum albumin (HSA) play crucial roles in the metabolism, distribution, and efficacy of platinum-based anticancer drugs. Polynuclear monofunctional platinum(II) complexes represent a new class of anticancer agents that display distinct molecular characters of pharmacological action from those of cisplatin. In this study, the interaction between a trinuclear monofunctional platinum(II) complex, $[Pt_3LCl_3](ClO_4)_3$ (L = *N*,*N*,*N*′,*N*′,*N*″,*N*″-hexakis(2-pyridylmethyl)-1,3,5-tris(aminomethyl)benzene) (**1**), and HSA was investigated using ultraviolet−visible spectroscopy, Fourier transform infrared spectroscopy, circular dichroism spectroscopy, fluorescence spectroscopy, molecular docking, and inductively coupled plasma mass spectrometry. The spectroscopic and thermodynamic data show that the interaction is a spontaneous process with the estimated enthalpy and entropy changes being 14.6 kJ mol^{-1} and 145.5 J mol^{-1} K^{-1}, respectively. The reactive sites of HSA to complex **1** mainly locate within its hydrophobic cavity in domain II. Noncovalent actions such as $\pi-\pi$ stacking and hydrophobic bonding are the primary contributors to the interaction between HSA and complex **1**, which is different from the scenario for cisplatin in similar conditions. The results suggest that the connection between complex **1** and HSA is reversible, and therefore the cytotoxic activity of the complex could be preserved during blood circulation.

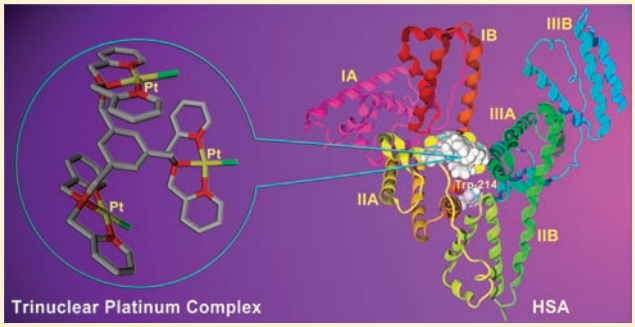

INTRODUCTION

Cellular resistance and systemic toxicity are two major defects of platinum-based anticancer drugs.[1] Platinum complexes with novel structures different from prototypical cisplatin have shown some favorable properties to overcome these shortcomings.[2] Polynuclear platinum(II) complexes represent a new class of anticancer agents with distinctive cytotoxic activities and different mechanism of action.[3,4] In the development of such complexes, we designed a trinuclear complex (**1**) using *N*,*N*,*N*′,*N*′,*N*″,*N*″-hexakis(2-pyridylmethyl)-1,3,5-tris(aminomethyl)benzene as a bridging ligand 5 years ago (Figure 1).[5] This complex demonstrated a higher cytotoxicity against the murine leukemia (P-388) and human non-small cell lung cancer (A-549) cell lines than that of cisplatin. Recently, we ascertained that complex **1** binds to DNA differently than cisplatin does, forming 1,3- and 1,4-intrastrand cross-links, as well as interstrand cross-links;[6] however, its behavior toward proteins is totally unknown.

Albumin is the principal extracellular protein, accounting for about 52% of the plasma proteins. Human serum albumin (HSA) consists of 585 amino acid residues organized in three domains (I, II, and III), each comprising two subdomains (A and B).[7] The main binding sites on HSA are located in hydrophobic cavities in subdomains IIA and IIIA, such as tryptophan (Trp-214) and tyrosine (Tyr-411) residues.[8] HSA bears negative charges at physiological pH (7.40) because of the ionization of amino acid residues (isoelectric point of HSA pI = 4.9) and tends to interact with positively charged species,[9]

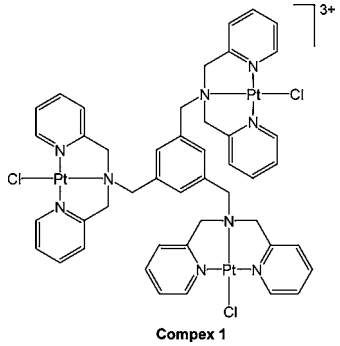

Figure 1. Molecular structure of complex **1**.

Received: August 6, 2011
Published: November 11, 2011

which means that HSA could exert a substantial impact on the transportation, distribution, and metabolism of pharmaceuticals.[8] The interactions of different platinum-based drugs with blood proteins, especially those with HSA, have received much attention in recent years.[10−12] These interactions may affect the concentration and deactivation of the platinum drugs, and thereby influence their availability and toxicity during chemotherapy.[13] For example, when cisplatin is introduced into the body intravenously, 50−61% of platinum is bound to HSA,[14] and the binding is essentially irreversible with less than 5% loss of bound-platinum after extensive dialysis.[15] However, the nature of the HSA−drug interactions remains unclear in many cases.[16] Therefore, studies on the molecular details of such interactions could deepen the understanding of platinum drugs and benefit the design of new platinum antitumor complexes.[17]

Various methods have been developed to study the interactions between platinum drugs and plasma proteins.[18] Nevertheless, most of the studies focus exclusively on the classical platinum drugs; while reports on "non-classical" polynuclear platinum(II) complexes are rather limited. In this paper, the interaction between complex **1** and HSA was investigated by ultraviolet−visible (UV−vis), Fourier transform infrared (FT-IR), circular dichroism (CD), and fluorescence spectroscopies, as well as molecular docking and inductively coupled plasma mass spectrometry (ICP-MS). The association constants, binding site, and acting forces between complex **1** and HSA were discussed on the basis of spectroscopic data.

EXPERIMENTAL SECTION

Materials. HSA (Fraction V powder, product number 1653, 96−99%) with a molecular mass of 66478 Da was purchased from Sigma and used without further purification. Complex **1** was prepared as described previously.[5] Tris(hydroxymethyl) aminomethane, bromophenol blue, and ibuprofen were obtained from Sigma. Common reagents were all of analytical grade. HSA solution (3.0 μM) was prepared with Tris−HCl buffer (0.05 M Tris, 0.1 M NaCl, pH 7.40). Phosphate buffer (0.02 M, pH 7.40) used in CD and FT-IR experiments was prepared with deionized water.

Equipments. UV−vis spectra were recorded at room temperature on a Perkin-Elmer Lambda 35 spectrometer equipped with quartz cells (1.0 cm). Fluorescence spectra were recorded on an LS−50B Spectrofluorimeter (Perkin−Elmer U.S.A.) equipped with quartz cells (1.0 cm) and a thermostat bath, setting the widths of both excitation and emission slits to 2.5 nm. Far-UV CD spectra were measured by a Jasco J-810 spectropolarimeter (Japan Spectroscopic, Japan) using a quartz cell (0.1 cm) at 0.1 nm intervals, adjusting the bandwidth to 1.0 nm and the scan speed to 20 nm min^{-1}. IR spectra of HSA solutions (15 μM) were recorded on a Bruker VECTOR22 spectrometer via the attenuated total reflection method with a resolution of 4 cm^{-1} and 60 scans. Pt analysis was performed on an inductively coupled plasma mass spectrometer (ICP-MS) using a standard Plasma-Quad II instrument (VG Elemental, Thermo Optek Corp.). The average of three independent results was taken as the final value.

Measurement Procedures. The concentration of HSA was fixed at 3.0 μM and that of complex **1** was varied from 1.5 to 15.0 μM in the fluorescence measurements. In the quenching experiments, HSA solutions were transferred into 5 mL volumetric flasks, and solutions of complex **1** with appropriate concentrations were added to the flasks, respectively. Fluorescence spectra (λ_{ex} = 280 nm, λ_{em} = 295−500 nm) were measured after the mixtures were incubated at 289, 299, and 309 K for 24 h, respectively. The scanning interval between excitation and emission wavelengths ($\Delta\lambda$) was stabilized at 15 or 60 nm. Three-dimensional (3D) fluorescence spectra were recorded under the following conditions: λ_{em} = 270−550 nm; λ_{ex} = 200 nm; scanning number, 15; and increment, 10 nm. Other parameters are the same as that in the quenching experiments.

The UV−vis spectra of complex **1** and HSA were recorded at room temperature. The CD spectra of HSA in the presence of complex **1** were recorded in the range of 200−250 nm, taking the average of three scans as the final data for each spectrum. The FT-IR difference spectrum of free HSA was acquired by subtracting the spectrum of the buffer solution from that of the protein solution; and the spectrum of the HSA−complex **1** system was obtained by subtracting the spectrum of complex **1** from that of the mixture.

In the ICP-MS measurement, complex **1** (1.2 mM) in Tris−HCl buffer solution was added to HSA (0.4 mM) such that their final concentrations reached 0.6 and 0.2 mM, respectively. The mixture reacted at 37 °C, and an aliquot of the solution (100 μL) was taken out at 0, 0.5, 2, 6, 12, 24, and 36 h, respectively. Each sample was centrifuged through a Microcon YM-10 membrane filter at 14000 *g* for 30 min. The isolated ultrafiltrate was digested with concentrated HNO_3 at 95 °C for 2 h, H_2O_2 at 95 °C for 1.5 h, and concentrated HCl at 37 °C for 0.5 h, sequentially. The solution was diluted to 5 mL with water, and the content of Pt was measured.

Molecular Docking. Molecular docking was carried out using software Autodock 4.2.3. The geometry of complex **1** was optimized by Gaussian 03 according to its crystal structure. The crystal data of HSA was obtained from the Protein Data Bank (PDB ID: 109X). Small molecules in HSA-109X were removed prior to the docking by software PyMOL. To recognize the binding sites in HSA, the grid size was set to 100, 100, and 100 along the *X*-, *Y*-, and *Z*-axes with a 0.375 Å grid spacing. Docking simulations were performed using the Lamarckian genetic algorithm (LGA) and the Solis and Wets local search method. Each run of the docking operation was terminated after a maximum of 2500000 energy evaluations.

RESULTS AND DISCUSSION

Fluorescence Spectroscopy. Fluorescence spectroscopy is an effective method to study the interactions of small molecules with HSA.[11,12] The fluorescence of Trp-214 may change when HSA interacts with other molecules, which could be reflected in the fluorescence spectra of HSA in the UV region.[19] The effect of complex **1** on the fluorescence intensity of HSA is shown in Figure 2. The intensity of the characteristic broad emission band at 345 nm decreases regularly with the increasing concentration of **1**, which indicates that some interactions between **1** and HSA have occurred. When the molar ratio of HSA to complex **1** reaches 1:60, the decrease in fluorescence intensity stops, suggesting that the HSA binding with complex **1** is fully saturated. The variation in intensity may

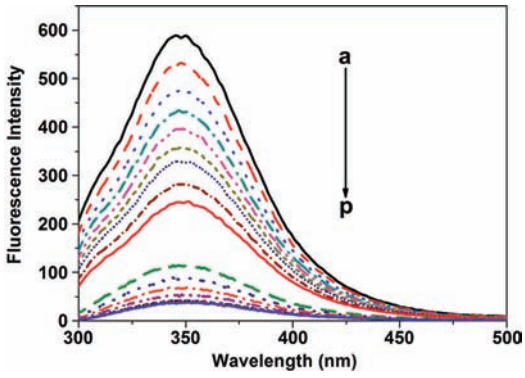

Figure 2. Effect of complex **1** (lines a−p: 0, 1.5, 3.0, 4.5, 6.0, 7.5, 9.0, 12.0, 15.0, 30.0, 60.0, 90.0, 120.0, 150.0, 180.0, and 210.0 μM, respectively) on the fluorescence spectra of HSA (3.0 μM, λ_{ex} = 280 nm) at 299 K and pH 7.40.

dx.doi.org/10.1021/ic201712e | *Inorg. Chem.* 2011, 50, 12661−12668

result from the changed protein conformation or direct quenching effect by complex **1**. Nevertheless, the maximum emission wavelength of HSA remained unchanged during the interaction, suggesting that Trp-214 did not undergo any change in polarity, and hence the complex was likely to interact with HSA via the hydrophobic region located inside the protein.[19]

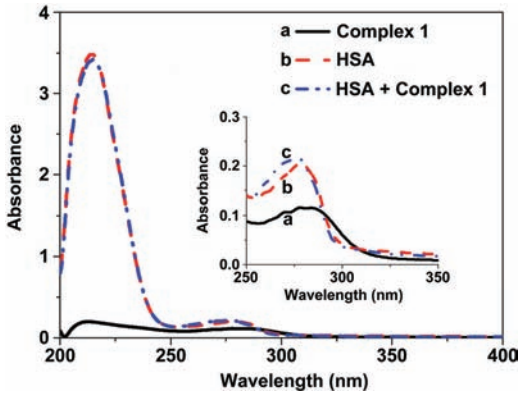

Figure 3. Absorption spectra of complex **1** (6.0 μM), HSA (3.0 μM), and HSA plus complex **1** (6.0 μM). Line (c) is a difference spectrum where the absorption of complex **1** in the buffer has been subtracted.

UV–vis Spectroscopy. UV–vis absorption measurement is a simple and applicable method to study the interactions between HSA and foreign species. Figure 3 shows the absorption spectra of HSA before and after the addition of complex **1**. The strong absorption peak at 214 nm originates from the n→π* transition of C═O in the backbone of HSA; the weak absorption peak at 277 nm arises from the phenyl rings in Trp, Tyr and phenylalanine (Phe) residues. When HSA is mixed with complex **1**, the intensity of the peak at 214 nm decreases while that of the peak at 277 nm increases to some extent, indicating that complex **1** can interact with HSA and the peptide strands of HSA are extended.[11] However, the maximum absorption wavelength remains unchanged, implying that the reaction between **1** and HSA is a noncovalent interaction in nature. Such an interaction may occur through the π–π stacking between aromatic rings of complex **1** and phenyl rings of Trp, Tyr and Phe residues located in the binding cavity of HSA. Since these residues possess conjugated π–electrons, they are inclined to share electrons with other π–systems.

CD Spectroscopy. CD measurement was performed in the presence of complex **1** at different concentrations to examine its possible impact on the secondary structure of HSA. As Figure 4 shows, two negative bands at 208 and 222 nm assignable to π→π* and n→π* transfers, respectively, are observed in the CD spectrum of HSA, which are characteristic of α-helical proteins.[20] The ellipticity of HSA decreases moderately with the increase in concentration of complex **1**, indicating some loss of α-helical secondary structure. This may imply that complex **1** is able to interact with the amino acid residues of the main polypeptide chain of HSA and partially destroy the hydrogen bonding networks. However, the CD spectra with or without complex **1** are similar in shape, suggesting that α-helix is still the predominant conformation of HSA in this system.

FT-IR Spectroscopy. The effect of complex **1** on the molecular structure of HSA was further assessed by FT-IR spectroscopy. Infrared spectra of proteins generally exhibit a

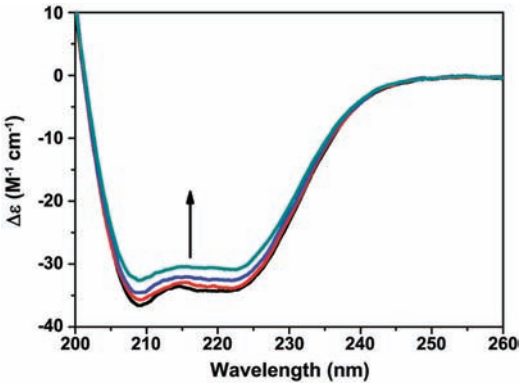

Figure 4. Far-UV CD spectra of HSA (3.0 μM) in the absence and presence of complex **1** (0, 3.0, 15.0, and 30 μM, respectively, from the bottom to the top).

number of so-called amide bands which represent different vibrations of the peptide moiety. Among them, amide I band is most sensitive to the changes of amide bonds in peptide chains and hence is widely used to study the secondary structure of proteins. The amide I band originates from the C═O

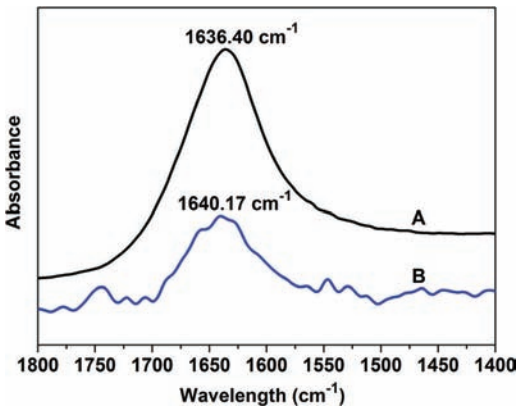

Figure 5. FT-IR difference spectrum of the amide I band of HSA (15.0 μM) (A) and that in the presence of complex **1** (15.0 μM) (B) in aqueous buffer solution (pH 7.40).

stretching vibration of the amide group and gives rise to infrared absorption in the region of about 1600–1700 cm^{-1}.[21] As Figure 5 shows, the amide I band of HSA only displays a moderate shift from 1636.40 to 1640.17 cm^{-1}, suggesting that complex **1** indeed exerts some influence on the polypeptide carbonyls of HSA, but the effect is rather weak and not likely to be a covalent binding. The decrease in intensity of the amide I band in the presence of complex **1** is due to the reduction of protein α-helical structure, which is consistent with the above CD spectra analysis.

Synchronous Fluorescence Spectroscopy. The molecular environment near the fluorophore was studied by synchronous fluorescence spectroscopy. In this method, the sensitivity associated with fluorescence is maintained while the spectrum is simplified, the spectral bandwidth is reduced, and different perturbing effects are avoided. When the scanning interval between excitation and emission wavelengths ($\Delta\lambda$) is stabilized at 15 and 60 nm, the spectrum provides the particular information of Tyr and Trp residues in a protein, respectively.[20] Therefore, the change in polarity around the fluorophore could be estimated by the shift in the maximum emission wavelength.

dx.doi.org/10.1021/ic201712e | *Inorg. Chem.* 2011, 50, 12661–12668

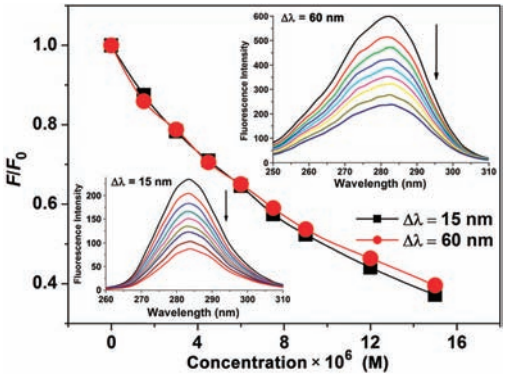

Figure 6. Impact of complex **1** (0, 1.5, 3.0, 4.5, 6.0, 7.5, 9.0, 12.0, and 15.0 μM from the top to the bottom, respectively) on the synchronous fluorescence spectra of HSA (3.0 μM) at different $\Delta\lambda$ values.

The synchronous fluorescence spectra of HSA in the presence of different concentrations of complex **1** are shown in Figure 6. The maximum emission wavelengths of Tyr and Trp residues are almost unchanged during the interaction, suggesting that the polarity around these residues is retained. However, a similar fluorescence quenching profile is observed for both Tyr and Trp residues upon addition of complex **1** to HSA. Tyr residues such as Tyr-263, 319, 332, 334, 341, 353, and 370 are located in domain II of HSA with a hydrophobic environment; and Trp-214 is also located in this domain. The fluorescence changes suggest that the interaction between complex **1** and HSA may occur in domain II, involving Tyr and Trp residues and inducing the quenching of fluorescence. This is different from the results observed for cisplatin, where the emission wavelength of HSA red-shifted during the interaction and cisplatin bound to HSA mainly through covalent bonds.[13] Since the spectroscopic changes of HSA induced by complex **1** are smaller than those by cisplatin, the association of complex **1** with HSA should be noncovalent and reversible.

3D Fluorescence Spectroscopy. 3D fluorescence spectroscopy is a newly emerged analytical technique that can provide more detailed information about the conformational changes of proteins. Figure 7 presents the 3D fluorescence spectra and the corresponding contour maps of HSA in the absence and presence of complex **1**, respectively. Peak 1 and peak 2 are the Rayleigh scattering peak ($\lambda_{ex} = \lambda_{em}$) and the second-ordered scattering peak ($\lambda_{em} = 2\lambda_{ex}$), respectively. Peak A (280, 346 nm, λ_{ex}, λ_{em}) reveals the spectral behavior of Trp and Tyr residues; and its condition is closely related to the microenvironmental polarity around these residues. Peak B (230, 342 nm, λ_{ex}, λ_{em}) mainly reflects the fluorescence character of the polypeptide backbone structure.[22] As Figure 7B shows, the fluorescence intensity of peaks A and B decreases significantly, though to a different extent, in the presence of complex **1**; as a result, the intensity ratios of peak A to peak B go up (Table 1). The decrease in peak A suggests that complex **1** could induce some conformational changes in HSA which are related to the hydrophobic microenvironment near Trp and Tyr residues. The decrease in peak B demonstrates that the structure of the peptide strands has changed after the addition of complex **1**, which agrees with the decrease of α-helix in the CD spectra. From these results, we deduce that HSA experienced a slight unfolding of the polypeptides in the presence of complex **1**.

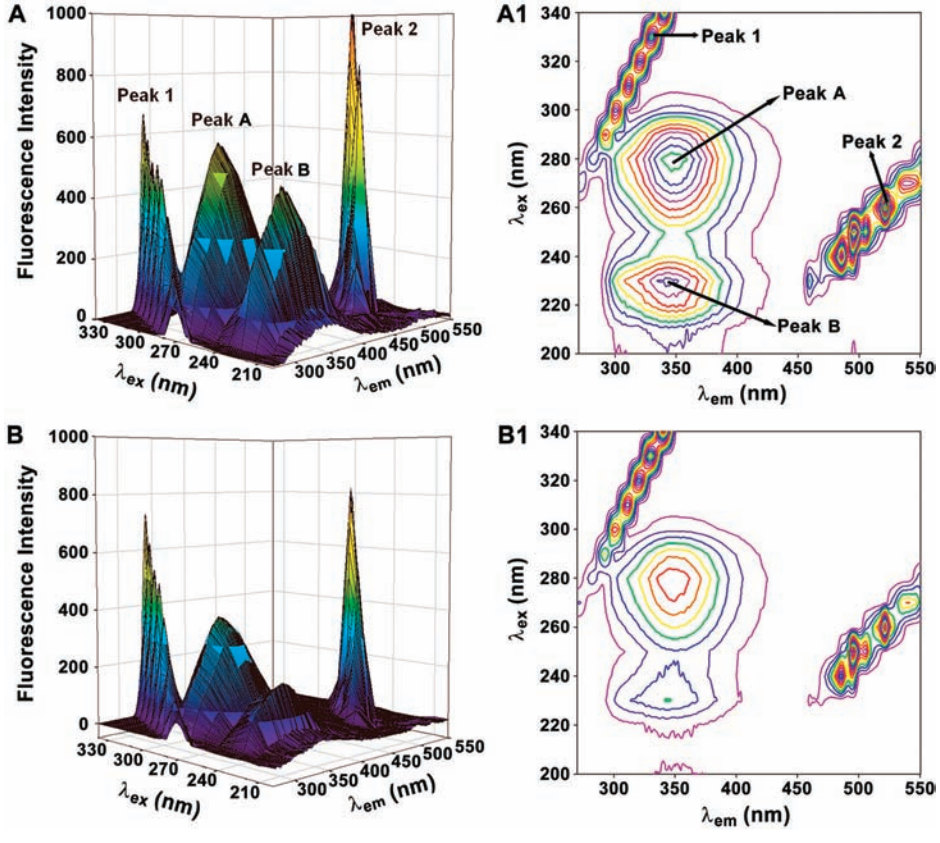

Figure 7. 3D projections and corresponding contour spectra of HSA (3.0 μM) in the absence (A, A1) and presence (B, B1) of complex **1** (6.0 μM).

dx.doi.org/10.1021/ic201712e | Inorg. Chem. 2011, 50, 12661–12668

Table 1. 3D Fluorescence Spectral Parameters of HSA in the Absence and Presence of Complex 1

system	peak A ($\lambda_{ex}/\lambda_{em}$)	$\Delta\lambda$ (nm)	intensity (peak A)	peak B ($\lambda_{ex}/\lambda_{em}$)	$\Delta\lambda$ (nm)	intensity (peak B)	intensity (A:B)
HSA	280/346	66	590.5	230/342	112	476.9	1.24:1
HSA + **1** (1:2)	280/346	66	390.6	230/344	114	202.8	1.93:1
HSA + **1** (1:5)	280/348	68	237.6	235/349	114	96.6	2.46:1

Fluorescence Quenching Mechanism. A spectral overlap between the fluorescence spectrum of HSA and the UV−vis

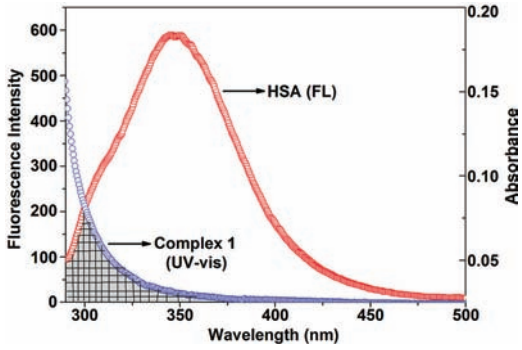

Figure 8. Overlap between the fluorescence emission spectrum of HSA (3.0 μM) and the UV−vis absorption spectrum of complex **1** (3.0 μM).

spectrum of complex **1** is shown in the shadowed part of Figure 8. The salient overlap suggests that there is a direct resonance energy transfer between HSA and complex **1**.

According to the Förster's theory, the energy transfer efficiency (E) is defined by eq 1:[23]

$$E = \frac{R_0^6}{R_0^6 + r^6} = 1 - \left(\frac{F}{F_0}\right) \tag{1}$$

where r is the distance between HSA (donor) and complex **1** (acceptor), R_0 is the Förster critical distance when the efficiency of energy transfer is 50%, F and F_0 are the fluorescence intensities of HSA in the presence and absence of complex **1**, respectively. R_0 can be calculated from eq 2:

$$R_0 = 0.211(k^2 n^{-4} \Phi J)^{1/6} \tag{2}$$

where k^2 is the spatial orientation factor between the emission dipole of HSA and absorption dipole of complex **1**, n is the average refractive index of the medium, Φ is the fluorescence quantum yield of HSA, and J is the overlap integral of the emission spectrum of HSA and the absorption spectrum (295−500 nm) of complex **1**, which could be obtained on eq 3:

$$J = \frac{\int_0^\infty F(\lambda)\,\varepsilon(\lambda)\lambda^4\,d\lambda}{\int_0^\infty F(\lambda)\,d\lambda} \tag{3}$$

where $F(\lambda)$ is the fluorescence intensity of HSA in the wavelength range from λ to $\lambda + \Delta\lambda$, $\varepsilon(\lambda)$ is the molar extinction coefficient of complex **1** at λ.

For a solution with random orientation as in this case, k^2 = 2/3, n = 1.36, and Φ = 0.15; accordingly, R_0 = 2.64 nm, E = 0.20, and r = 3.33 nm. The distance between HSA and complex **1** is less than 7 nm, indicating that a static quenching interaction has occurred.[23]

Further, the fluorescence quenching mechanism can be described by the Stern−Volmer equation:[24]

$$\frac{F_0}{F} = 1 + K_{sv}[Q] = 1 + K_q\tau_0[Q] \tag{4}$$

where K_{sv} is the Stern−Volmer constant, [Q] is the concentration of complex **1**, K_q is the quenching rate constant of HSA, and τ_0 is the lifetime of HSA without complex **1**, respectively. Obviously,

$$K_q = K_{sv}/\tau_0 \tag{5}$$

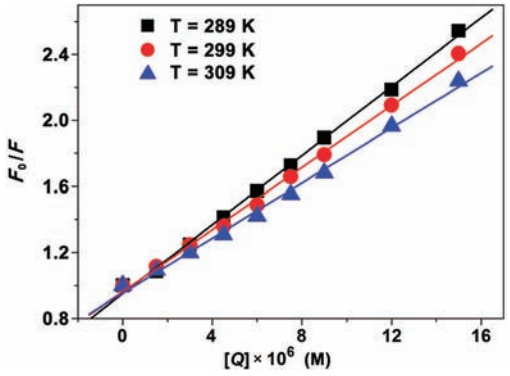

Figure 9. Stern−Volmer plots for quenching of HSA (3 μM) fluorescence by complex **1** at different concentrations and temperatures (pH 7.40, λ_{ex} = 280 nm, λ_{em} = 345 nm).

The Stern−Volmer plots of HSA in the presence of complex **1** at different concentrations and temperatures are shown in Figure 9. The linearity of the plots is independent of the temperature. When the concentration of HSA was fixed, K_{sv}

Table 2. Stern−Volmer Constants and the Quenching Rate Constants of HSA in the Presence of Complex 1 (pH 7.40)

T (K)	$K_{sv} \times 10^{-5}$ (M^{-1})	$K_q \times 10^{-13}$ (M^{-1} s^{-1})	R[a]	SD[b]
289	1.04 ± 0.02	2.08 ± 0.04	0.999	0.0251
299	0.94 ± 0.02	1.88 ± 0.04	0.998	0.0270
309	0.83 ± 0.02	1.66 ± 0.04	0.998	0.0304

[a]The correlation coefficient. [b]The standard deviation.

could be obtained from the slope of the regression curves. For HSA, τ_0 is approximately 5 ns;[24] thus K_q was obtained. The calculated constants for the interaction are listed in Table 2. Since the maximum value of K_q for a diffusion-controlled quenching process is about 10^{10} M^{-1} s^{-1}, the higher K_q values ($\sim 10^{13}$ M^{-1} s^{-1}) presented here suggest that the quenching of Trp fluorescence occurred via a specific interaction between HSA and complex **1**, and static quenching is the dominant mechanism.[25] Moreover, the Stern−Volmer quenching constant K_{sv} is inversely correlated with the temperature, which indicates that the fluorescence quenching of HSA by complex **1** is not a dynamic process but a static process.

Interaction Characters. For a static quenching process, the association constant (K_A) and the number of binding sites (n) can be calculated using eq 6:[26]

dx.doi.org/10.1021/ic201712e | Inorg. Chem. 2011, 50, 12661−12668

$$\log \frac{F_0 - F}{F} = n \log K_A - n \log\left(\frac{1}{[Q_t] - (F_0 - F)[P_t]/F_0}\right) \quad (6)$$

where F_0 and F are the fluorescence intensities in the absence and presence of complex **1**, respectively; $[Q_t]$ and $[P_t]$ are the total concentrations of complex **1** and HSA, respectively. Figure

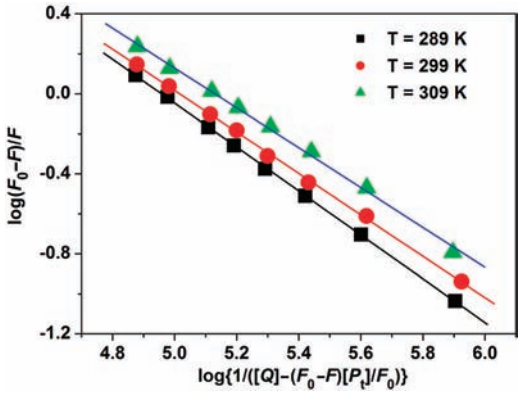

Figure 10. Plots of $\log(F_0 - F)/F$ versus $\log\{1/([Q_t] - (F_0 - F)[P_t]/F_0)\}$ at different temperatures for HSA (3.0 μM, pH 7.40) in the presence of complex **1** (λ_{ex} = 280 nm, λ_{em} = 345 nm).

10 shows the plots of $\log (F_0 - F)/F$ versus $\log \{1/([Q_t] - (F_0 - F)[P_t]/F_0)\}$ for the interaction between HSA and complex **1** at different temperatures. K_A and n obtained from the plots are listed in Table 3. The association constants increase with the temperature, suggesting that the interaction is an endothermic process. The number of binding site in HSA approximates to 1, indicating that only one site in HSA is reactive to complex **1**. By contrast, several binding sites, including Cys-34, Met-298, 329, Tyr-150 or 148, His-67, 247 and Asp-375 residues, are involved in the interaction of HSA with cisplatin via covalent bonds.[14] Therefore, the interaction of HSA with complex **1** is relatively weaker than that with cisplatin.

Four types of interactions, that is, hydrogen bond, hydrophobic interaction, van der Waals interaction, and ionic interaction, may be related to the noncovalent protein association reactions.[27] To clarify the major interaction mode, thermodynamic parameters, $\Delta G°$, $\Delta H°$, and $\Delta S°$, of the reaction were calculated from the Van't Hoff eqs 7 and 8:[11]

$$\ln K_A = -\Delta H°/RT + \Delta S°/R \quad (7)$$

$$\Delta G° = \Delta H° - T\Delta S° \quad (8)$$

where K_A is the association constant at temperature T, and R is the gas constant. The calculated enthalpy ($\Delta H°$), free energy ($\Delta G°$), and entropy ($\Delta S°$) changes are summarized in Table 3. The negative value of $\Delta G°$ indicates that the interaction of complex **1** with HSA is spontaneous. The values of both $\Delta H°$ and $\Delta S°$ are positive, which suggests that the contributions to these changes arise from hydrophobic and ionic interactions.[27] Complex **1** contains seven aromatic rings and exists in solution as a cation; therefore, hydrophobic interactions and $\pi-\pi$ stacking with amino acid residues such as Trp, Tyr, and His in HSA are reasonable, and electrostatic interactions are also justifiable. In contrast with cisplatin that mainly forms irreversible adducts with HSA through covalent bonds,[13] complex **1** reacts with HSA via noncovalent interactions and hence the association is reversible.

Binding Site of HSA for Complex 1. Trp-214 is highly sensitive to its local environment, and changes in its emission spectra often occur in response to conformational transitions, subunit association, substrate binding, or denaturation.[24] Chemical-induced protein denaturation usually leads to increased exposures of Trp, Tyr, and Phe residues to water, which cause changes in their fluorescence, especially for that of Trp-214. Guanidine hydrochloride (GnHCl) is a chemical denaturant often used to induce unfolding of the multidomain proteins. When the concentration of GnHCl is below 1.8 M, only domain III of HSA unfolds completely with no changes in either helical content or the native conformation of domains I and II; when the concentration is above 1.8 M, domains I and II begin to unfold and separate from each other.[28] To clarify the binding site of HSA for complex **1**, the impact of **1** on the fluorescence spectra of HSA in the presence of GnHCl was measured. As Figure 11 shows, at 1.5 M GnHCl, domain III of

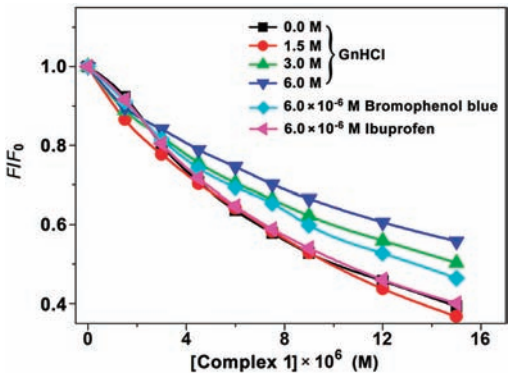

Figure 11. Changes in the HSA (3.0 μM) fluorescence induced by complex **1** in the presence of GnHCl, bromophenol blue, and ibuprofen, respectively (pH 7.40, λ_{ex} = 280 nm, λ_{em} = 345 nm).

HSA has been completely unfolded; however, the fluorescence changes induced by **1** are almost the same as those without GnHCl. The result indicates that the unfolding of domain III does not affect the interaction between **1** and HSA, and therefore the primary binding site for complex **1** may not lie in this domain. At 3.0 and 6.0 M GnHCl, domains I and II have been unfolded largely and completely, respectively,[28] and the fluorescence quenching is reduced obviously because of the

Table 3. Association Constants and Thermodynamic Parameters for the Interaction between HSA and Complex 1 at Different Temperatures

T (K)	$K_A \times 10^{-5}$ (M^{-1})	n	$\Delta H°$ (kJ mol^{-1})	$\Delta G°$ (kJ mol^{-1})	$\Delta S°$ (J mol^{-1} K^{-1})
289	0.91 ± 0.02	1.10 ± 0.01	14.6 ± 0.0	−27.4 ± 0.2	145.5 ± 0.7
299	1.11 ± 0.01	1.03 ± 0.00		−28.9 ± 0.2	
309	1.35 ± 0.02	1.00 ± 0.02		−30.4 ± 0.2	

dx.doi.org/10.1021/ic201712e | Inorg. Chem. 2011, 50, 12661−12668

resurgent Tyr fluorescence in denatured HSA. However, Trp-214 is still close to complex **1** so that the fluorescence is quenched to some extent.[23] The result suggests that complex **1** may react with Trp-214 in the subdomain IIA of HSA. Since the spectral characters of Trp-214 did not change much under these conditions as compared with that in native HSA, the association between HSA and complex **1** is most likely maintained through noncovalent interactions.

Ligand competition experiments were performed to further identify the primary binding site of HSA for complex **1**. There are two main binding sites in HSA, that is, site I locating in subdomain IIA and site II existing in subdomain IIIA.[29] Bromophenol blue and ibuprofen were thus selected for the experiments because they have shown high affinity for site I (K = 1.5 × 10^6 M^{-1}) and site II (K = 2.7 × 10^6 M^{-1}), respectively.[30] As shown in Figure 11, the fluorescence of HSA induced by complex **1** is evidently affected by bromophenol blue but not by ibuprofen, indicating that the site I in domain II is the primary reactive site for the association of HSA with complex **1**. Generally, the primary binding sites of HSA for a metal complex is chiefly determined by the nature of the chelating ligand, which can direct the metal to a specific site in the protein. The hydrophobic ligand of complex **1** could facilitate platinum(II) to enter the hydrophobic domain II of HSA and thereby promote the interaction.

Molecular docking was performed to understand the binding affinity and mode between complex **1** and HSA. The blind docking mode with the lowest binding free energy is shown in Figure 12. Complex **1** is surrounded by Lys-195, 274, 444, Arg-218, 222, Asn-295, Cys-278, 289, 448, Glu-292, 294, Val-293, His-440, Pro-447, Asp-451, and Tyr-452. The interaction occurs in the area between subdomains IIA and IIIA, but mainly in IIA. Complex **1** partly enters subdomain IIA, resulting in the fluorescence quenching of Trp-214. A $\pi-\pi$ stacking exists between phenyls of complex **1** and Tyr-452 in HSA. The interaction energies between amino residues and complex **1** are listed in Table 4. The data indicate that Glu-294, Val-293, Glu-292, and Arg-222 in subdomain IIA as well as Asp-451 and Cys-448 in subdomain IIIA interact effectively with complex **1**. Hydrophobic interactions between complex **1** and Val-293 or Pro-447 are involved in the association, but hydrogen bonds are not involved in the interaction. The simulation results coincide well with the above thermodynamic analysis.

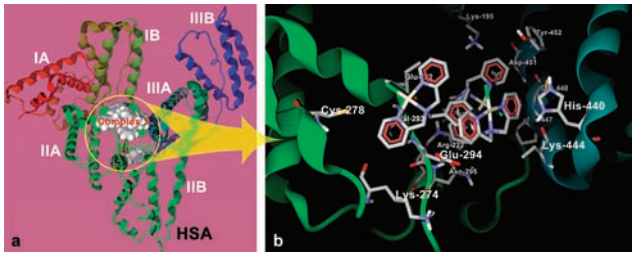

Figure 12. Docking of complex **1** in the active site of HSA. (a) The full view of **1** in HSA with the complex and Trp-214 being depicted in space-filling representation; (b) detailed illustration of the surroundings nearby complex **1** in HSA.

Inductively Coupled Plasma Mass Spectrometry (ICP-MS). Finally, to evaluate and quantitate the association of complex **1** with HSA, the unbound ultrafilterable protein fraction was determined by ICP-MS after the complex was incubated with HSA for different times. As shown in Figure 13,

Table 4. Interaction Energies between Complex 1 and Responsive Amino Acid Residues in Molecular Docking[a]

amino acid residues	interaction energy (kJ mol^{-1})
Arg-218	−2.097
Arg-222	−11.101
Asn-295	−3.114
Asp-451	−12.226
Cys-278	−1.354
Cys-289	−3.048
Cys-448	−10.865
Glu-292	−15.006
Glu-294	−38.784
His-440	−9.442
Lys-195	−2.110
Lys-274	−3.472
Lys-444	−8.128
Pro-447	−3.782
Tyr-452	−7.144
Val-293	−19.758

[a]The MolDock score and ReRank score are −182.03 and −86.25, respectively.

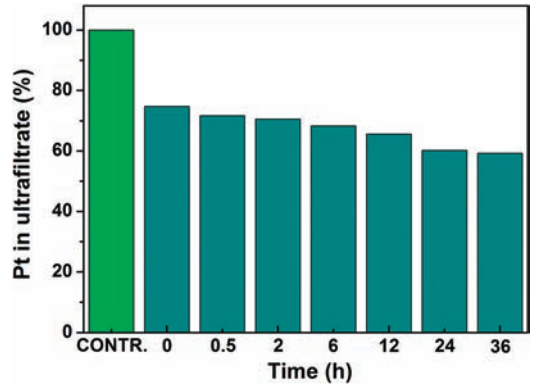

Figure 13. ICP-MS analysis of Pt content in the ultrafiltrate after complex **1** was incubated with HSA for different periods of time.

the Pt content in the ultrafiltrate decreases (~25%) immediately (t = 0) upon complex **1** mixing with HSA, which could be ascribed to the "pre-association" or noncovalent interactions of the complex with protein.[31] However, further decrease is limited (~10%) throughout 36 h after the initial preassociation, suggesting that covalently bound Pt−HSA species are not formed during the interaction. This means that if complex **1** is delivered though vein infusion, nonprotein-bound drug would be able to diffuse readily to tissues without losing activity. The conclusion also accords with the results obtained from above spectroscopic studies.

■ CONCLUSIONS

Interactions of polynuclear platinum complexes with proteins are of great importance for understanding the biochemical fate of platinum drugs in vivo. This paper reports our investigation of the interactions of a trinuclear platinum complex (**1**) with HSA using various methods. The association between complex **1** and HSA is essentially sustained by noncovalent interactions, where hydrophobic interaction and $\pi-\pi$ stacking play pivotal roles. Noncovalent interactions with HSA are favorable for the availability of platinum drugs to tumor cells because they do not compromise the DNA binding ability of the drugs during

dx.doi.org/10.1021/ic201712e | Inorg. Chem. 2011, 50, 12661−12668

delivery. In this case, HSA may function as a "passive" drug carrier and the HSA−complex **1** system may serve as a drug reservoir for the therapeutic purpose. These results are beneficial to understanding the antitumor activity and toxicity of polynuclear monofunctional platinum(II) complexes.

AUTHOR INFORMATION

Corresponding Author

*E-mail: boxwxy@nju.edu.cn (X.W.), zguo@nju.edu.cn (Z.G.).

ACKNOWLEDGMENTS

The financial support from the National Basic Research Program of China (Grant 2011CB935800) and the National Natural Science Foundation of China (Grants 90713001, 30870554, 21021062, and 21131003) are gratefully acknowledged.

REFERENCES

(1) Wang, X. Y.; Guo, Z. J. *Dalton Trans.* **2008**, 1521−1532.
(2) Wang, X. Y. *Anti-Cancer Agents Med. Chem.* **2010**, *10*, 396−411.
(3) Fan, D. M.; Yang, X. L.; Wang, X. Y.; Zhang, S. C.; Mao, J. F.; Ding, J.; Lin, L. P.; Guo, Z. J. *J. Biol. Inorg. Chem.* **2007**, *12*, 655−665.
(4) Lin, M. X.; Wang, X. Y.; Zhu, J. H.; Fan, D. M.; Zhang, Y. M.; Zhang, J. F.; Guo, Z. J. *Apoptosis* **2011**, *16*, 288−300.
(5) Zhao, Y. M.; He, W. J.; Shi, P. F.; Zhu, J. H.; Qiu, L.; Lin, L. P.; Guo, Z. J. *Dalton Trans.* **2006**, 2617−2619.
(6) Zhu, J. H.; Zhao, Y. M.; Zhu, Y. Y.; Wu, Z. Y.; Lin, M. X.; He, W. J.; Wang, Y.; Chen, G. J.; Dong, L.; Zhang, J. F.; Lu, Y.; Guo, Z. J. *Chem.—Eur. J.* **2009**, *15*, 5245−5253.
(7) Dockal, M.; Carter, D. C.; Rüker, F. *J. Biol. Chem.* **1999**, *274*, 29303−29310.
(8) He, X. M.; Carter, D. C. *Nature* **1992**, *358*, 209−215.
(9) Leis, D.; Barbosa, S.; Attwood, D.; Taboada, P.; Mosquera, V. *Langmuir* **2002**, *18*, 8178−8185.
(10) Mandal, R.; Kalke, R.; Li, X.-F. *Chem. Res. Toxicol.* **2004**, *17*, 1391−1397.
(11) Yue, Y. Y.; Chen, X. G.; Qin, J.; Yao, X. J. *Colloids Surf., B* **2009**, *69*, 51−57.
(12) Lemma, T.; Pawliszyn, J. *J. Pharm. Biomed. Anal.* **2009**, *50*, 570−575.
(13) Espósito, B. P.; Najjar, R. *Coord. Chem. Rev.* **2002**, *232*, 137−149.
(14) Hu, W.; Luo, Q.; Wu, K.; Li, X.; Wang, F.; Chen, Y.; Ma, X.; Wang, J.; Liu, J.; Xiong, S.; Sadler, P. J. *Chem. Commun.* **2011**, *47*, 6006−6008.
(15) Ivanov, A. I.; Christodoulou, J.; Parkinson, J. A.; Barnham, K. J.; Tucker, A.; Woodrow, J.; Sadler, P. J. *J. Biol. Chem.* **1998**, *273*, 14721−14730.
(16) Timerbaev, A. R.; Hartinger, C. G.; Aleksenko, S. S.; Keppler, B. K. *Chem. Rev.* **2006**, *106*, 2224−2248.
(17) Cummings, S. D. *Coord. Chem. Rev.* **2009**, *253*, 1495−1516.
(18) Bischin, C.; Lupan, A.; Taciuc, V.; Silaghi-Dumitrescu, R. *Mini-Rev. Med. Chem.* **2011**, *11*, 214−224.
(19) Froehlich, E.; Mandeville, J. S.; Jennings, C. J.; Sedaghat-Herati, R.; Tajmir-Riahi, H. A. *J. Phys. Chem. B* **2009**, *113*, 6986−6993.
(20) Ibrahim, N.; Ibrahim, H.; Kim, S.; Nallet, J.-P.; Nepveu, F. *Biomacromolecules* **2010**, *11*, 3341−3351.
(21) Khan, S. N.; Islam, B.; Yennamalli, R.; Sultan, A.; Subbarao, N.; Khan, A. U. *Eur. J. Pharm. Sci.* **2008**, *35*, 371−382.
(22) Zhang, Y.-Z.; Zhou, B.; Liu, Y.-X.; Zhou, C.-X.; Ding, X.-L.; Liu, Y. *J. Fluoresc.* **2008**, *18*, 109−118.
(23) Abou-Zied, O. K.; Al-Shihi, O. I. K. *J. Am. Chem. Soc.* **2008**, *130*, 10793−10801.
(24) Lakowicz, J. R. *Principles of Fluorescence Spectroscopy*, 3rd ed., Springer: New York, 2006.
(25) Shang, L.; Wang, Y. Z.; Jiang, J. G.; Dong, S. J. *Langmuir* **2007**, *23*, 2714−2721.
(26) Bi, S. Y.; Song, D. Q.; Tian, Y.; Zhou, X.; Liu, Z. Y.; Zhang, H. Q. *Spectrochim Acta A* **2005**, *61*, 629−636.
(27) Ross, P. D.; Subramanian, S. *Biochemistry* **1981**, *20*, 3096−3102.
(28) Ahmad, B.; Ahmed, M. Z.; Haq, S. K.; Khan, R. H. *Biochim. Biophys. Acta* **2005**, *1750*, 93−102.
(29) Caravan, P.; Cloutier, N. J.; Greenfield, M. T.; McDermid, S. A.; Dunham, S. U.; Bulte, J. W. M.; Amedio, J. C. Jr.; Looby, R. J.; Supkowski, R. M.; Horrocks, W. D. Jr.; McMurry, T. J.; Lauffer, R. B. *J. Am. Chem. Soc.* **2002**, *124*, 3152−3162.
(30) Tinoco, A. D.; Eames, E. V.; Incarvito, C. D.; Valentine, A. M. *Inorg. Chem.* **2008**, *47*, 8380−8390.
(31) Montero, E. I.; Benedetti, B. T.; Mangrum, J. B.; Oehlsen, M. J.; Qu, Y.; Farrell, N. P. *Dalton Trans.* **2007**, 4938−4942.